

1 Modern Physics Letters A
 Vol. 25, No. 17 (2010) 1–19
 3 © World Scientific Publishing Company



5 **SEARCHES FOR NEW PHYSICS WITH JETS-PLUS- \cancel{E}_T
 SIGNATURES USING DATA-DRIVEN BACKGROUND
 ESTIMATES**

7 PIERRE-HUGUES BEAUCHEMIN

9 *Particle Physics Sub-Dept., University of Oxford, Denys Wilkinson Building, Keble Road,
 Oxford, OX1 3RH, UK
 h.beauchemin@physics.ox.ac.uk*

11 PIERRE SAVARD

13 *Department of Physics, University of Toronto,
 60 St. George St. Toronto, Ontario M5S 1A7, Canada
 savard@physics.utoronto.ca*

15 Received 12 April 2010

17 Events featuring high energy jets and a large amount of missing transverse energy con-
 19 stitute a key signature for a wide spectrum of new physics models. In this review, the
 21 results of two searches with such signatures are presented. The benefits of perform-
 ing these searches in a model-independent way are discussed and data-driven techniques
 used to estimate Standard Model backgrounds are described in detail. These data-driven
 techniques will be an important part of searches for new physics at the LHC, especially
 in the early data-taking period.

23 *Keywords:* Jets-plus- \cancel{E}_T ; data-driven; model-independent.

25 **1. Introduction**

27 The Standard Model of particle physics provides an accurate description of the
 data collected so far by a wide variety of particle physics experiments. The ex-
 traordinary precision of many experimental results, such as electroweak parameter
 measurements, the anomalous magnetic moment of the electron ($g-2$) or the running
 of the strong interaction coupling constant (α_S)^{1,2} are a few examples that have
 confirmed Standard Model predictions at the level of small higher order quantum
 corrections. Despite this success, the Standard Model is considered by many high
 energy physicists as no more than an effective theory valid only below the TeV
 energy scale. The reason for this is that many fundamental questions about nature
 are not answered within the context of the Standard Model. For example, the SM
 does not explain the origin of the matter–anti-matter asymmetry of the Universe, it
 does not describe the gravitational interaction, and does not include a viable dark

2 *P.-H. Beauchemin & P. Savard*

1 matter particle. It also does not explain why the strong CP terms, *a priori* allowed
in the Standard Model Lagrangian, are so suppressed (strong CP problem)³ and
3 there is no natural mechanism that explains what keeps the Higgs boson mass at
the electroweak mass scale in the presence of very large higher order corrections.

5 In the past few decades, many different theories have been developed to address
some of the questions left unanswered within the Standard Model. The construc-
7 tion of these new physics theories are now severely constrained by existing mea-
surements in particle physics, astrophysics, and cosmology. They typically predict
9 the existence of new particles or interactions that would profoundly impact particle
physics phenomenology at the energy scale of electroweak symmetry breaking and
11 above. The study of this energy range could help us understand why this symmetry
is broken, and solve the naturalness problem of the Standard Model. Moreover, if
13 dark matter is made of Weakly Interacting Massive Particles (WIMPs), the mass
of these particles would have to be close to this energy range.⁴ The Tevatron Col-
15 lider and the Large Hadron Collider are able to probe this energy scale and their
experiments are in a position to reveal new phenomena should they be close to the
17 electroweak breaking scale.

19 Discrepancies with SM expectations could manifest themselves in a variety of
ways including production cross sections, branching ratios, or more complex re-
21 lationships between different measurable quantities (e.g. unitarity of the CKM
triangle). A key advantage of the high energy hadron colliders mentioned above
is their potential to directly produce these new particles which is why they are
23 often referred to as “discovery machines”. This direct observation of new particles
is to be contrasted with their indirect observation which would manifest itself in
25 discrepancies in some SM parameter values. The simplest case of the observation of
a new particle is a resonance in the invariant mass distribution obtained from the
27 reconstruction of all of its decay products. A more challenging case involves final
states with undetectable particles. Here, the missing information becomes “missing
29 transverse energy” or \cancel{E}_T , and results in an incomplete kinematic reconstruction
of the event preventing the use of the invariant mass as a discriminating variable.
31 Also, the missing momentum potentially opens the door to additional instrumen-
tal backgrounds that require dedicated efforts to understand and control. It is this
33 challenge of finding new physics in final states with jets and missing momentum
that will be addressed in this review.

35 After a brief survey of some new physics models that can be used as benchmarks
to interpret the results of searches in jets-plus- \cancel{E}_T final states, we will present data-
37 driven techniques that can be used to estimate the Standard Model background
to jets-plus- \cancel{E}_T events. Example of such searches for new physics conducted at the
39 Tevatron will be used to illustrate the use of data-driven techniques to estimate
the major Standard Model backgrounds.⁵⁻⁷ The result of these searches and their
41 interpretation will then be presented in Sec. 5.

1 2. Jets-Plus- \cancel{E}_T Searches

3 Final-state signatures featuring energetic jets and a large amount of missing trans-
 4 verse energy have a great potential for new physics discoveries. A large variety of
 5 new physics scenarios, including supersymmetry,^{8,9} extra dimensions^{10–12} and lep-
 6 toquarks,^{13,14} predict enhanced contributions of jets-plus- \cancel{E}_T events compared to
 7 SM predictions. In general, any model predicting associated production of partons
 8 and weakly interacting particles or pair production of unstable particles whose de-
 9 cay products are a single parton and a non-interacting particle could be observed
 10 as an excess of events above the Standard Model expectation in the jets-plus- \cancel{E}_T
 11 channels.

12 Large amounts of missing transverse energy in these new physics signals could
 13 be produced by Standard Model particles like neutrinos. For example, leptoquarks
 14 decaying to a quark and a neutrino would produce jets-plus- \cancel{E}_T events.^{13,14} The
 15 missing momentum could also come from particles not included in the Standard
 16 Model like gravitons which could escape into extra dimensions.^{10–12} If the non-
 17 interacting particle is protected against eventual decay by a discrete symmetry like
 18 the R -parity conservation in supersymmetry,^{15,16} or the KK-number conservation
 19 in Universal Extra Dimension scenarios^{17,18} or T-parity conservation in smallest
 20 Higgs models,¹⁹ it would be stable and therefore a candidate for a dark matter
 21 particle.

22 The production of particles in the new physics models described above generally
 23 involves the strong interaction which implies high production rates. The fact that
 24 new physics events with jets-plus- \cancel{E}_T are expected to be produced at a high rate at
 25 hadron colliders and that these events could feature dark matter particles justify
 the importance assigned to these searches at hadron colliders.

2.1. Signature-based searches

26 As discussed above, many final state signatures can be used to search for a wide
 27 range of new physics models. However, the sensitivity associated with the choice of
 28 the kinematic phase space will be model-dependent: the maximisation of the sensi-
 29 tivity to a specific new physics model can lead to very different choices of kinematic
 30 selections depending on the model considered. This optimisation approach is not
 31 necessarily the one best suited to find new physics beyond the Standard Model.
 32 In general, we are more interested in ruling out the Standard Model than we are
 33 interested in ruling out any given particular new physics scenario. There are so
 34 many models that predict significant contributions to a jets-plus- \cancel{E}_T final state,
 35 that optimising selections on any one of them could reduce our chances to find
 36 new physics at all. There are generally no good reasons to favour one model over
 37 others, especially since the models that are often available in Monte Carlo based
 38 calculations are essentially toy models that are not realistic, even if the underlying
 39 theory is potentially correct.

4 *P.-H. Beauchemin & P. Savard*

1 The idea of signature-based searches is to keep the highest possible indepen-
3 dence with respect to theoretical models by choosing event selections based mainly
5 on experimental criteria rather than *a priori* optimisation for a given new physics
7 model. The choice of selection cuts for this approach will be limited more by exper-
9 imental considerations rather than any particular theoretical considerations. This
11 approach will not yield a sensitivity to new physics that is as high as a dedicated
13 search for a given model. However, such a generic search is less likely to miss a new
15 physics signal. Furthermore, should an actual excess be observed, dedicated searches
17 would typically not be in a position to claim evidence for the particular model that
19 was searched for without ruling out other possible alternatives for the excess and
21 without looking at many other final states. Therefore, searches for new physics
23 performed in a model-independent way in many exclusive final states represent a
25 better strategy for understanding the nature of potential non-SM contributions.

27 In the end, if no significant excess over Standard Model expectations is observed,
29 results can be used to set constraints on a wide variety of new physics models. In
31 general the limits can be set on a simple benchmark model as it provides a good
33 reference with which similar measurements could be compared to.

3. Data-driven Background Calculations

35 The sensitivity to potential new physics depends not only on the number of new
37 physics and background events but also on the precision of the background esti-
39 mate. Therefore, a key element to control in order to maximise our sensitivity to
41 the numerous new physics scenarios is the precision with which the background is
43 estimated. Many systematic uncertainties, such as those coming from the jet en-
45 ergy scale and resolution effects, the detector acceptance and efficiency estimates,
47 and the modelling of underlying event and parton distribution functions, will be
49 relatively large in the early data-taking period of the LHC experiments. Analy-
51 ses designed to minimise the impact of these uncertainties will in general be more
53 robust. Such robust analyses can be achieved by using data-driven estimates of
55 the Standard Model contributions to the signature under study. These techniques
57 should therefore play an important role in searches for new physics, both at the
59 Tevatron and the LHC.

3.1. *Motivation for data-driven estimate of jets-plus- \cancel{E}_T backgrounds*

61 Typically, Standard Model predictions for final states involving jets and \cancel{E}_T suffer
63 from large systematic uncertainties due to effects that are hard to model prop-
65 erly in simulation. These effects can be divided into two categories: non-calculable
67 contributions to the prediction and detector modelling.

69 The production of jets, due to the confined nature of the strong interaction,
71 involves non-perturbative processes which cannot be predicted by the usual tech-
73 niques used in quantum field theory. The general procedure is to start from the

1 well-understood perturbative calculation performed in the centre-of-mass of the
parton (quark and gluons) system and then to add effects that account for the
3 parton density function of the colliding hadrons (protons or anti-protons), the po-
tential gluon emissions of the initial state or final state partons, the hadronisation
5 of the final partons to create jets of colourless hadrons, and the other potential
partonic collisions that can occur within the same colliding hadrons. Most of these
7 effects cannot be computed within the quantum chromodynamic theory and require
approximate models for which a large number of parameters need to be tuned to
9 experimental data. Despite this tuning, the uncertainty due to the approximate
modelling of these effects can have a large impact on the predicted production of
11 jets. Moreover, such tuning is performed in a jet kinematic phase space region which
is different from the one that is probed for the new physics searches motivated above.
13 Using data events containing jets with similar kinematics to predict the Standard
Model contribution will reduce significantly the impact of uncertainties associated
15 with the modelling of such non-perturbative effects.

The second important factor which contributes to the uncertainty on the pre-
17 dicted background is the imperfect modelling of the calorimeter response to jets.
Although the simulation will in general reproduce well the energy scale and res-
19 olution on average, the inadequate modelling of calorimeter cracks, dead regions,
particle punch-through, and rare fragmentation effects will lead to large tails in the
21 \cancel{E}_T distribution.

For all the above reasons, the exclusive use of Monte Carlo simulation to predict
23 the Standard Model contribution to jets-plus- \cancel{E}_T events can result in large system-
atic uncertainties. However, using data itself for a Standard Model prediction can
25 greatly reduce many of the systematic uncertainties mentioned above. For example,
if the calibration of the energy of jets was off by 10%, both the prediction and the
27 observation would be off by the same amount and the difference between the Stan-
dard Model prediction and the observation would remain unaffected. Calibrating a
29 prediction on data is therefore a robust way to minimise resulting jet energy scale
and resolution uncertainties.

31 From these considerations, we can see that the objective of data-driven esti-
mates of Standard Model backgrounds is to significantly reduce the systematic
33 uncertainty on the predictions by using some well-identified data sample to model
the background rather than relying on Monte Carlo modelling of the above effects.
35 In particular, the idea here is to find a data sample orthogonal to the jets-plus- \cancel{E}_T
final state (control region), but similar enough to be able to provide a good model
37 of the shape of the jet energy or \cancel{E}_T distributions. The sources of uncertainty on
such estimates would therefore essentially be reduced to the statistics of the con-
39 trol regions data. If such background estimate techniques are an asset for mature
experiments like CDF and D0, they are even more desirable for newly experiments
41 like ATLAS and CMS for which Monte Carlo simulation have not yet been tuned
to collider data.

6 *P.-H. Beauchemin & P. Savard*

1 The use of such data-driven estimates will be advantageous provided that the
 3 choice of the control region does not introduce significant biases on kinematic dis-
 tributions, and that sufficiently large statistical samples can be found such that the
 5 normalisation can be estimated precisely. The following sections will illustrate how
 this can be done with examples of data-driven estimates of the electroweak and
 QCD backgrounds for searches for new physics performed at CDF.

7 **4. Jets-Plus- \cancel{E}_T Searches with CDF**

Two examples of analyses performed at the Tevatron will be presented in the fol-
 9 lowing section. Although the details of the selection cuts will be different from one
 experiment to the next, the overall strategy and techniques are applicable in general
 11 to hadron collider experiments.

4.1. Event selections and non-collision backgrounds

13 The cases of one jet (monojet) and two jets plus \cancel{E}_T (dijet+ \cancel{E}_T) analyses are dis-
 15 cussed below. Although both measurements feature different final states and are sen-
 sitive to different new physics processes, most of the event selections can be applied
 to both analyses. For example, in both measurements, jets are reconstructed with
 17 a cone-based algorithm using a cone size of $\Delta R = \sqrt{\Delta(\eta)^2 + \Delta(\phi)^2} =$
 0.7 .^{20,a} Only jets with a E_T threshold of 20 GeV after the application of jet en-
 19 ergy scale corrections²¹ were considered for these analyses. The monojet analysis
 requires exactly one of those jets while the dijet+ \cancel{E}_T analysis requires exactly two
 21 jets. Events for which the \cancel{E}_T points in the direction of a jet in ϕ are rejected to re-
 duce the QCD background. The requirement is that the difference in the azimuthal
 23 angle ϕ between the \cancel{E}_T and each jet satisfies $\Delta(\phi_{E_T} - \phi_{\text{jet}}) \geq 0.5$ rad. In order to
 reduce the W+jets background, a lepton veto is applied. This veto rejects events in
 25 which an isolated track of $P_T \geq 10$ GeV is reconstructed. The isolation requirement
 is defined by the fraction of the energy contained in a cone of 0.4 centred on the
 27 track which has to be less than 10% of the transverse momentum of that track. To
 further reduce the electron contribution, none of the selected jets must have more
 29 than 90% of their energy contained in the electromagnetic calorimeter.

Cosmic rays, beam-gas collisions and beam halo events can contribute to the
 31 monojet and dijet+ \cancel{E}_T signatures. They are the largest source of background to the
 monojet final state without the “cleanup” cuts described below. It is sufficient for a
 33 cosmic ray muon or a beam halo muon produced upstream of the detector to cross
 the calorimeter and emit large bremsstrahlung radiation to obtain a large deposition

^aWe use a coordinate system where θ is the polar angle to the proton beam, ϕ is the azimuthal
 angle about this beam axis, and η is the pseudorapidity defined as $-\ln \tan(\theta/2)$. The missing
 transverse energy, \cancel{E}_T , is then defined as the magnitude of $-\sum_i E_T^i \hat{n}_i$ where \hat{n}_i is a unit vector
 in the azimuthal plane that points from the beamline to the i th calorimeter tower and E_T^i is the
 transverse component of measured energy in the tower, defined as $E^i \cdot \sin(\theta)$.

1 of energy in the calorimeter which will yield a jet signature, and by construction,
 2 a correlated equal amount of \cancel{E}_T . This kind of background is relatively hard to
 3 predict, even from Monte Carlo simulation, and therefore requires an extra set of
 4 selections, to maximally reduce its contribution. This non-collision background gets
 5 almost completely eliminated by requiring that:

- 6 • a reconstructed primary vertex with at least five tracks pointing to it and within
 7 60 cm of the centre of the detector;
- 8 • the sum of the transverse momentum of the tracks matched to each jet fiducial
 9 to the tracker be at least 10% of the jet transverse energy;
- 10 • the leading jet is central ($|\eta| < 1.0$);
- 11 • there is at least 10% of the total energy deposited in the full calorimeter which
 12 is contained in the electromagnetic component of the calorimeter.

13 Timing information available from the hadronic calorimeter has been used to es-
 14 timate the small, residual non-collision background. The number of jets-plus- \cancel{E}_T
 15 events for which the time of a significant energy deposition in the calorimeter is not
 16 synchronised with the nearest collision is compared with the number of such events
 17 in W/Z+jets events to set an upper limits in the residual non-collision background.
 18 The cosmic ray background is therefore estimated by a data-driven method. After
 19 the cleanup cuts are applied, physics backgrounds (electroweak and QCD multijets)
 20 need to be tackled next.

21 **4.2. QCD multijets background**

22 QCD multijet events can become a background to jets-plus- \cancel{E}_T searches if one or
 23 more jets are badly mis-measured. This background would dominate the electroweak
 24 backgrounds without the requirement that the \cancel{E}_T vector does not point in the
 25 direction of any jet. After this selection the QCD background is not expected to
 26 be large based on the MC simulation. For the MC simulation to be used, however,
 27 we must trust its ability to accurately model detector cracks and uninstrumented
 28 regions, and to model the fragmentation that leads to jets that have very few
 29 particles which can more easily generate missing transverse energy. In the analyses
 30 described here, data-driven techniques have been chosen to estimate this source of
 31 background.

32 After the selection above, a QCD multijet event will become a background if at
 33 least one of the jets in the event is completely lost, i.e. loses enough energy to fall
 34 below the jet counting threshold. We can therefore classify the QCD background
 35 in two orthogonal categories:

- 36 • Category A: events where one jet is dominantly responsible for the observed \cancel{E}_T .
 37 In those events, the \cancel{E}_T would point in the direction of the jet, if it was not lost.
- 38 • Category B: events where at least two jets significantly contribute to the \cancel{E}_T . In
 39 those events, the \cancel{E}_T does not point in the general direction of any jet.

8 *P.-H. Beauchemin & P. Savard*

1 According to the Monte Carlo simulation, category A dominates for low mul-
2 tiplicity jets-plus- \cancel{E}_T final states (less than four jets). For this reason, the general
3 strategy is to use the data to estimate the absolute contribution of the dominant
4 category A events and use the MC simulation to calculate the small residual cate-
5 gory B contribution.

6 In order to estimate the category A background with n -jets+ \cancel{E}_T events, events
7 are selected that have $(n + 1)$ -jets+ \cancel{E}_T . For these events, one of the jets points in
8 the direction of the \cancel{E}_T . These events are orthogonal and unbiased with respect
9 to the signal events, and can therefore be used for the data-driven estimate of the
10 QCD multijet background. By studying the transverse energy distribution of that
11 jet as more and more of the jet transverse energy is lost, we can estimate how many
12 events will have jets below the jet counting threshold. This can be done by fitting
13 the E_T distribution of this jet and doing an extrapolation below the jet count-
14 ing threshold using the fit. This is the region populated with QCD background
15 events of category A. To avoid double counting of the electroweak background,
16 the W/Z+jets contribution to the fitted data must be removed. Such a correction
17 generally amounts to 15–20% of the overall prediction for the QCD background
18 of category A. Once the correction for electroweak contamination is applied, the
19 integral of the extrapolated function in the signal region provides the data-driven
20 estimate for this background. An example of a fitted distribution for the corrected
21 data, taken from the CDF monojet search for new physics, is shown in Fig. 1. In
22 this example, the jet counting threshold was set to 20 GeV, although the method
23 has been redone with a threshold of 15 GeV, as can be seen on the figure, to test
24 that the method works well. The predicted number of QCD background events of
25 category A, extracted from the extrapolation of Fig. 1, is 591 ± 87 events. The
26 quoted uncertainty of 15% accounts for the statistics of the control region, the
27 systematic uncertainty on the fit and its extrapolation, and the systematic uncer-
28 tainty on the electroweak contamination correction. The contribution of category
29 B events still needs to be evaluated. Similar data-driven methods to estimate the
30 QCD background to jets-plus- \cancel{E}_T events could not be applied on the QCD back-
31 ground of category B. This is because there is no way to build a control region
32 which would not get important contributions from the signal region. At the LHC,
33 attempts to use the category A control region to construct a \cancel{E}_T transfer function
34 that could be applied to estimate the background of category B is under study.
35 In the analyses described here, the Monte Carlo simulation was used to estimate
36 the relative contribution of category B events over category A events. The use of
37 the ratio reduces the expected systematic uncertainty but because of the low MC
38 statistics left after all cuts and the small impact of the category B contribution
39 on the overall jets-plus- \cancel{E}_T measurements, a conservative 100% uncertainty on the
40 relative contribution of the category B background was used. For example, in the
41 CDF monojet analysis, the relative contribution of category B events was estimated
42 to $20 \pm 20\%$, for an overall prediction of 708 ± 146 QCD background events.

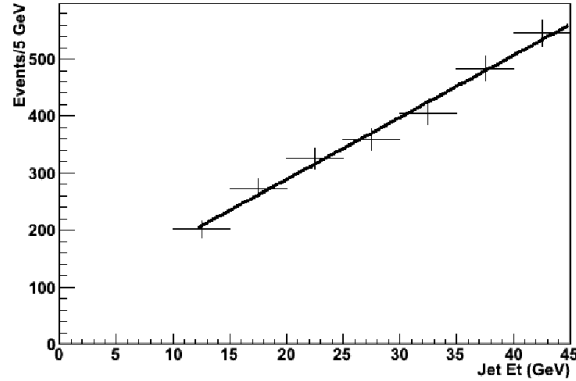


Fig. 1. Transverse energy of the second most energetic jet of multijet data events. There is no lepton in these events and the large \cancel{E}_T points in the direction of the sub-leading jet. The extrapolation of the fitted distribution below 20 GeV is used for the QCD background estimate to 80 GeV monojet events.

1 4.3. Electroweak backgrounds

After the application of cleanup selections and the substantial reduction in the QCD background thanks to the $\Delta\phi$ cut, the remaining background will be from electroweak processes. In particular, the largest source of Standard Model background to jets-plus- \cancel{E}_T events is predicted to come from Z+jets events, where the Z-boson decays to a pair of neutrinos and W+jets events where the W decays to a lepton (e , μ or τ) that is not observed in the detector, i.e. escaping our lepton veto requirements. To estimate these backgrounds, we can use Z+jets and W+jets events for which the leptons (e or μ) are well reconstructed and identified rather than being vetoed, and on which the “+jets” requirement corresponds to the exactly same set of selections applied in the jets-plus- \cancel{E}_T searches. It is because the jet selections are the same for the signal (jets-plus- \cancel{E}_T) and control regions and that they are applied on the same type of processes (W/Z+jets) that the data-driven estimates are less affected by large systematic uncertainties which would result from the modelling of jet quantities. These control region events therefore satisfy important criteria for data-driven background estimates. First, they use an orthogonal data sample to the signal sample. Because of the lepton selections, they do not contain any contamination from the jets-plus- \cancel{E}_T events selected in the signal region. Second, the shape of the jets and \cancel{E}_T distributions are not biased by the choice of the control sample. This has been checked in the simulation and in the data by varying kinematic selections. In order to get the \cancel{E}_T distribution of Z($\rightarrow \nu\nu$)+jets events from Z($\rightarrow \ell\ell$)+jets events, the energy of the measured charged leptons has to be removed from the event. Since the impact of the lepton energy scale and resolution uncertainties on the \cancel{E}_T measurement is much smaller than the same uncertainties for jets, the lepton removal procedure does not induce noticeable biases on the modelling of the Z($\rightarrow \nu\nu$)+jets \cancel{E}_T distribution.

1 In order to be able to use these distributions to estimate the electroweak back-
 3 ground to jets-plus- \cancel{E}_T events, they must be properly normalised. These normali-
 5 sation factors will vary depending on whether the distributions from the controlled
 7 regions are used to estimate the $Z(\rightarrow \nu\nu)$ +jets events or if they are used to estimate
 9 $W(\rightarrow \ell\nu)$ +jets events where the charged lepton is lost. In both cases, a correction
 to the distribution normalisation must be made for the lepton acceptance (A_{lept})
 as well as for the lepton trigger, reconstruction and identification efficiencies (ϵ_{lept}).
 Of course, these efficiencies are different for W and Z events, because they involve
 a different number of charged leptons.

The second important contribution to the normalisation factor that needs to
 be computed is the estimate of the Standard Model background to the W/Z+jets
 events selected in the control regions. For example, QCD multijet events for which
 one of the jets fully mimics the signature of an electron will contribute to the $W \rightarrow$
 $e\nu$ +jets distributions used to estimate the jets-plus- \cancel{E}_T background, without being a
 background to jets-plus- \cancel{E}_T events itself. It has been verified that these backgrounds
 to $W \rightarrow \ell\nu$ +jets or $Z \rightarrow \ell\ell$ +jets events do not noticeably distort the shape of the
 jet energy or \cancel{E}_T distributions extracted from the W/Z+jets event candidates. This
 is because of the way they are selected and the smallness of their contribution
 ($\sim 20\%$ of the total $W(\rightarrow e\nu)$ +jets events, and $\sim 5\%$ of the $Z(\rightarrow ee)$ +jets events
 for example). Their impact on the final prediction is therefore essentially just a
 change in the normalisation. To limit the effect of these backgrounds on the overall
 systematic uncertainty of the measurement, data-driven techniques have been used
 to estimate the contribution of the QCD background to W/Z+jets events.

Once the above normalisation corrections are applied, we obtain a measurement
 of $W \rightarrow \ell\nu$ +jets and $Z \rightarrow \ell\ell$ +jets cross sections for the same jet selections to
 those that are probed in the jets-plus- \cancel{E}_T searches. An estimate of the $Z \rightarrow \nu\nu$ +jets
 background to jets-plus- \cancel{E}_T events can thus be obtained from the $Z \rightarrow \ell\ell$ +jets cross
 section measurements by multiplying this measured cross section by the ratio of
 $Z \rightarrow \nu\nu$ to $Z \rightarrow \ell\ell$ branching ratios as measured at LEP: $\frac{\text{Br}(Z \rightarrow \nu\nu)}{\text{Br}(Z \rightarrow ee)} = 5.942 \pm 0.018$.¹
 However, before obtaining the final $Z \rightarrow \nu\nu$ +jets background prediction, there is
 another correction factor that needs to be included in the normalisation calculation
 to account for small differences in the geometrical jet acceptance of the $Z \rightarrow \ell\ell$ +jets
 cross section measurement, compared to the geometrical volume available to jets
 in $Z \rightarrow \nu\nu$ events. This is because the removal of charged leptons from the event,
 which is done in order to calculate the \cancel{E}_T , reduces the geometrical volume available
 for jets. The jet acceptance therefore differs slightly and a correction ($A_{\text{jets}}^{\text{corr}}$) must
 be added, in order to get a correct prediction for the $Z \rightarrow \nu\nu$ +jets background.
 The following equation summarises how the $Z \rightarrow \nu\nu$ +jets background prediction is
 obtained from $Z \rightarrow \ell\ell$ +jets events passing the same jet selections as those applied
 in the jets-plus- \cancel{E}_T searches ($N_{Z(\rightarrow \ell\ell)+\text{jets}}$):

$$N(Z \rightarrow \nu\nu + \text{jet}) = 5.942 \times \frac{N_{Z(\rightarrow \ell\ell)+\text{jets}} - N_{\text{bkg}}}{A_{\text{lept}} \times \epsilon_{\text{lept}}} \times A_{\text{jets}}^{\text{corr}} \times \epsilon_{\text{trig}} \times \frac{L_{\text{trig}}}{L_{\text{lept}}}, \quad (1)$$

Table 1. Normalisation factors estimated for $Z \rightarrow \ell\ell+1$ -jets cross section measurements ($\ell = e$ or μ) when the jet transverse energy and the \cancel{E}_T are above 80 GeV. The numbers are for 1.1 fb^{-1} of CDF run II data. Note that here, the acceptance includes a Monte Carlo-based efficiency correction. To reflect the data-driven estimate of the lepton selection efficiencies, we also quote the scale factor ($\epsilon_{\text{lept}}^{\text{SF}} = \frac{\epsilon_{\text{lept}}^{\text{Dat}}}{\epsilon_{\text{lept}}^{\text{MC}}}$) that need to be applied to the quoted acceptances.

Normalisation factors	$Z \rightarrow ee+1$ -jets	$Z \rightarrow \mu\mu+1$ -jets
Raw data events ($N_{Z(\rightarrow\ell\ell)+\text{jets}}$)	112	100
Acceptance ($A_{\text{lept}} \times \epsilon_{\text{lept}}^{\text{MC}}$)	0.156 ± 0.006	0.240 ± 0.007
Efficiency SF ($\epsilon_{\text{lept}}^{\text{SF}}$)	1.017 ± 0.010	0.923 ± 0.023
Background (N_{bkg})	3 ± 3	negligible
Jets acceptance corr. ($A_{\text{jets}}^{\text{corr}}$)	0.957 ± 0.027	1.120 ± 0.025
\cancel{E}_T trigger efficiency (ϵ_{trig})	0.993	0.993
Luminosity correction ($\frac{L_{\text{trig}}}{L_{\text{lept}}}$)	0.887	0.930
$Z \rightarrow \nu\nu+1$ -jets estimate	3470 ± 377	2798 ± 296

1 where ϵ_{trig} is the efficiency of the trigger (jet or \cancel{E}_T triggers) used to gather the
 jets-plus- \cancel{E}_T data sample, L_{trig} is the integrated luminosity of this sample, and
 3 L_{lept} is the integrated luminosity of the sample collected with the lepton triggers.
 Table 1 gives an example of these normalisation corrections in the context of a
 5 $Z \rightarrow \nu\nu+\text{jets}$ background estimate for monojet events where both the leading jet
 transverse energy and the \cancel{E}_T of the events (after lepton removal) are above 80 GeV.
 7 As can be seen in the table, the total uncertainty on the number of $Z \rightarrow \nu\nu+\text{jets}$
 events predicted is higher than 10%, while the total uncertainty from each of the
 9 normalization factors adds up to less than 6%. The difference is due to the limited
 $Z \rightarrow \ell\ell+\text{jets}$ statistics available for the high kinematic region.

11 There is an order of magnitude more $W \rightarrow \ell\nu+\text{jets}$ than $Z \rightarrow \ell\ell+\text{jets}$ events. If
 the $W \rightarrow \ell\nu+\text{jets}$ events could be exploited to obtain a prediction for $Z \rightarrow \nu\nu+\text{jets}$
 13 events, the total uncertainty on the prediction would be significantly reduced. To
 do this, the ratio R_{jets} of $W \rightarrow \ell\nu+\text{jets}$ to $Z \rightarrow \ell\ell+\text{jets}$ cross sections is used. This
 15 ratio is calculated at Next-to-Leading order in perturbation theory and the resulting
 systematic uncertainties are relatively small. It should be noted that the use of the
 17 ratio cancels some of the uncertainties of the individual cross section calculations.
 By computing this ratio for the phase space regions under study, a $Z \rightarrow \nu\nu+\text{jets}$
 19 prediction can be obtained from $W \rightarrow \ell\nu+\text{jets}$ events. For example, in the $W/Z+1$ -
 jet case where the jet transverse energy and the \cancel{E}_T are above 80 GeV, theoretical
 21 calculations performed with the MCFM program²² yield $R_{\text{jets}} = 9.0 \pm 0.3$. Applying
 the normalisation correction procedure outlined above on $W \rightarrow \ell\nu+\text{jets}$ events gives
 23 a total of four statistically independent estimates for the $Z \rightarrow \nu\nu+\text{jets}$ background
 to jets-plus- \cancel{E}_T events. The details of the estimate from $W+\text{jets}$ events for the CDF

Table 2. Normalisation factors estimated for $W \rightarrow \ell\nu+1$ -jets cross section measurements ($\ell = e$ or μ) when the jet transverse energy and the \cancel{E}_T are above 80 GeV. The numbers are for 1.1 fb^{-1} of CDF run II data. Note that here, the acceptance includes a Monte Carlo-based efficiency correction. To reflect the data-driven estimate of the lepton selection efficiencies, we also quote the scale factor ($\epsilon_{\text{lept}}^{\text{SF}} = \frac{\epsilon_{\text{lept}}^{\text{Dat}}}{\epsilon_{\text{lept}}^{\text{MC}}}$) that need to be applied to the quoted acceptances.

Normalisation factors	$W \rightarrow e\nu+1$ -jets	$W \rightarrow \mu\nu+1$ -jets
Raw data events ($N_{W(\rightarrow\ell\nu)+\text{jets}}$)	1610	1299
Acceptance ($A_{\text{lept}} \times \epsilon_{\text{lept}}^{\text{MC}}$)	0.223 ± 0.006	0.244 ± 0.007
Efficiency SF ($\epsilon_{\text{lept}}^{\text{SF}}$)	0.965 ± 0.008	0.868 ± 0.005
Background (N_{bkg})	312 ± 47	232 ± 24
Jets acceptance corr. ($A_{\text{jets}}^{\text{corr}}$)	0.973 ± 0.026	1.055 ± 0.026
\cancel{E}_T trigger efficiency (ϵ_{trig})	0.993	0.993
Luminosity correction ($\frac{L_{\text{trig}}}{L_{\text{lept}}}$)	0.887	0.930
$Z \rightarrow \nu\nu+1$ -jets estimate	3440 ± 231	3267 ± 179

1 monojet search are given as an example in Table 2. As can be seen in Tables 1
 2 and 2, the four predictions are consistent within uncertainties. By combining them
 3 we obtain a final prediction of 3207 ± 138 $Z \rightarrow \nu\nu$ +jets background events. The
 4 relative uncertainty on this combined prediction using both W+jets and Z+jets
 5 events is two times smaller than what would be obtained from $Z \rightarrow \ell\ell$ +jets events
 6 alone, and about five time smaller than what would be obtained from Monte Carlo-
 7 based predictions.

8 Starting from the measurement of $W \rightarrow \ell\nu$ +jets cross sections, we can estimate
 9 the contribution of the other W/Z+jets backgrounds to the jets-plus- \cancel{E}_T candidate
 10 sample. To this end, one simply needs to estimate the fraction of events in which the
 11 charged lepton is not reconstructed, is outside of the detector acceptance or other-
 12 wise fails to be rejected by the lepton veto requirements. Such probability to “lose”
 13 the charged leptons ($P(\ell \rightarrow \cancel{\ell})$) must be estimated from Monte Carlo. However,
 14 by exploiting the relevant ratios of Monte Carlo events to obtain such estimate,
 15 systematic uncertainties due to non-perturbative QCD effects (e.g. hadronisation,
 16 PDF, etc.) or due to the modelling of detector effects does not significantly increase
 17 the overall uncertainty on the final prediction. Table 3 displays these probabilities
 18 that the lepton survives veto cuts for the various lepton types in the context of
 19 a CDF search for new physics in monojet events. As can be seen in the table,
 20 electrons are less likely to be lost than muons because of the wider coverage of
 21 the CDF calorimeter compared to its tracker. The fact that the tau background
 22 is the largest is a consequence of events where a tau fakes a jet object, enhancing
 23 their contribution to jets-plus- \cancel{E}_T events. Although the probability to lose the two
 charged leptons from $Z \rightarrow \ell\ell$ +jets events is small, their contribution to jets-plus- \cancel{E}_T

Table 3. Probability that all the charged leptons of a $W \rightarrow \ell\nu$ +jets or a $Z \rightarrow \ell\ell$ +jets event get lost, i.e. survive the lepton veto requirements, when the jet transverse energy and the \cancel{E}_T are above 80 GeV.

Processes	$P(e \rightarrow \cancel{e})$	$P(\mu \rightarrow \cancel{\mu})$	$P(\tau \rightarrow \cancel{\tau})$
$W \rightarrow \ell\nu$ +1-jets	$20.8 \pm 0.3\%$	$33.0 \pm 1.0\%$	$54.6 \pm 0.8\%$
$Z \rightarrow \ell\ell$ +1-jets	0.0%	$11.9 \pm 0.2\%$	$7.9 \pm 0.2\%$

1 events have been estimated in the same way as for the W+jets contribution. This
 2 completes the data-driven estimate of the electroweak backgrounds to jets-plus- \cancel{E}_T
 3 events which amounts to $\sim 90\%$ of the total background.

5. CDF Results

5 The data-driven ideas and techniques to estimate Standard Model backgrounds to
 6 jets-plus- \cancel{E}_T events have been used in CDF for monojet and dijet+ \cancel{E}_T signature-
 7 based searches for new physics. In order to illustrate how these methods perform
 8 in actual measurements, we report the results of these two searches. Examples of
 9 interpretations of the result obtained from the comparison of the predictions with
 the observations are also provided.

11 5.1. Monojet search

12 A background prediction for three different kinematic regions is obtained for the
 13 monojet analysis using the data-driven techniques presented above. This increases
 the sensitivity to different new physics scenarios, while keeping a model-independent
 15 approach. As mentioned before, two of those kinematic regions are determined
 from the trigger requirement that the \cancel{E}_T or jet triggers are fully efficient. As a
 17 consequence, a requirement of 80 GeV on the jet E_T and on the \cancel{E}_T is imposed on
 the monojet sample collected from the \cancel{E}_T trigger, while a jet of $E_T > 150$ GeV and
 19 120 GeV of \cancel{E}_T are required for monojet events collected from the jet trigger. A third
 region is probed based on the criteria that there are enough W/Z+jets events with a
 21 well-reconstructed lepton to perform a data-driven background estimate with 1 fb^{-1}
 of data. A jet of 180 GeV and an \cancel{E}_T of 150 GeV are then required to define this third
 23 kinematic region probed for new physics. As can be seen in Table 4, the observations
 in the three kinematic regions probed for new physics are consistent with Standard
 25 Model expectations obtained with the methods outlined above. Although the search
 performed consists in a counting experiment, a comparison between the observed
 27 and predicted \cancel{E}_T distributions for monojet events is provided in Fig. 2. It shows
 that the agreement between Standard Model predictions and the monojet data is
 good over the entire distribution. From these results, no evidence for new physics
 29 in 1 fb^{-1} was found in the CDF monojet data.

31 Although no new physics has been found with these monojet analyses, results
 can be used to constrain the parameters of different new physics scenarios which

Table 4. Estimated SM backgrounds and the number of observed monojet data events for 80/80 ($E_T > 80$ GeV, $\cancel{E}_T > 80$ GeV), 150/120 ($E_T > 150$ GeV, $\cancel{E}_T > 120$ GeV) and 180/150 ($E_T > 180$ GeV, $\cancel{E}_T > 150$ GeV) candidate samples.

Background	80/80	150/120	180/150
$Z \rightarrow \nu\nu + \text{jets}$	3207 ± 138	338 ± 30	139 ± 17
$W \rightarrow e\nu + \text{jets}$	1959 ± 67	187 ± 14	58 ± 5
$W \rightarrow \mu\nu + \text{jets}$	1530 ± 53	117 ± 9	35 ± 3
$W \rightarrow \tau\nu + \text{jets}$	808 ± 28	58 ± 4	18 ± 2
$Z \rightarrow \ell\ell + \text{jets}$	96 ± 4	8 ± 1	2 ± 0
QCD multi-jet	708 ± 146	23 ± 20	12 ± 12
$\gamma + \text{jets}$	209 ± 41	17 ± 5	8 ± 3
Non-collision	52 ± 52	10 ± 10	3 ± 3
Total expected	8564 ± 331	808 ± 62	275 ± 30
Data observed	8449	809	319

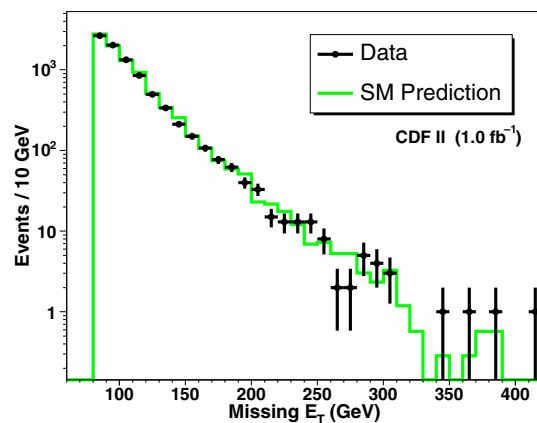


Fig. 2. Comparison of the event \cancel{E}_T for the 8449 events in the candidate sample used for the 80/80 monojet search for new physics with the predicted Standard Model distribution. The prediction does not include a systematic uncertainty on the shape of the Standard Model background distribution which is directly taken from Monte Carlo.

- 1 predict an enhanced monojet signal with respect to Standard Model predictions.
- From the number of observed events, the predicted number of Standard Model
- 3 background events, and the uncertainty on this background prediction, an upper
- limit on the number of new physics events contributing to our sample events can
- 5 be obtained. For example, in the 150/120 region, the measurement is consistent at
- 95% confidence level with a maximum of 125 new physics events. This number is
- 7 essentially model-independent and can be used to set limits on the parameters of
- any new physics model of interest.

Table 5. 95% C.L. lower limits on the fundamental Planck scale M_D in TeV obtained from the 150/120 monojet analysis as a function of $n = 2-6$ extra dimensions. Comparison with LEP results are also provided.

Extra dimensions	M_D (TeV)	
	CDF monojet	LEP combined
$n = 2$	1.33	1.60
$n = 3$	1.10	1.20
$n = 4$	0.99	0.94
$n = 5$	0.92	0.77
$n = 6$	0.89	0.66

1 Graviton production in the context of Large Extra Dimension (LED) models
 2 have been chosen as a benchmark model that can be constrained by the monojet
 3 measurement. After an *a priori* comparison, the 150/120 measurement was deter-
 4 mined to be the most sensitive to LEDs and therefore was used for the calculation
 5 of the limits on the fundamental Planck scale in $4 + n$ dimensions. To that end,
 6 the maximum number of new physics events obtained above can be converted into
 7 an upper limit on the monojet production cross section from LED models²³ after
 8 calculation of the signal acceptance. Monte Carlo simulations are used for this esti-
 9 mate. For example, in the case of two large extra dimensions, the signal acceptance
 10 is estimated to $9.9 \pm 1.3\%$. The uncertainty includes effects from the modelling of
 11 jet energy scale and resolution (8%), partons density function (6%), initial and final
 12 state radiation (3%) and integrated luminosity (6%). This systematic uncertainty is
 13 twice as large as the total uncertainty on the background prediction for the 150/120
 14 measurement, which is essentially all statistical. This illustrates the gain that can
 15 be obtained from using data-driven estimates of the Standard Model background.
 16 Note that this gain is larger for lower kinematic regions where the statistics of the
 17 control sample are larger. For example, in the region where both the jet E_T and
 18 the \cancel{E}_T are required to be above 8 GeV, the total uncertainty on the Standard
 19 Model background prediction is less than 4%, which is approximately a factor of
 20 four lower than what would have been obtained from Monte Carlo based predic-
 21 tions. This shows that the systematic uncertainty on background prediction is well
 22 controlled when this prediction is extracted directly from data. The upper limit
 23 on the graviton production cross section in the ADD scenario can then be used to
 24 constrain the fundamental Planck scale in $4 + n$ dimensions M_D . Table 5 presents
 25 the lower limit on M_D as a function of the number of large extra dimensions n , and
 26 is compared with LEP limits on M_D obtained from photon-plus- \cancel{E}_T events. LEP
 27 constraints are better than CDF limits for $n = 2$ and $n = 3$. However, these two
 28 cases are significantly disfavoured by astronomical considerations.²⁴⁻²⁷ The cases
 29 $n > 3$ are not disfavoured by astrophysics, and the CDF monojet results set the
 best constraints on the fundamental Planck scale M_D .

Table 6. Estimate SM of backgrounds and the number of observed dijet+ \cancel{E}_T event for loose ($H_T > 125$ GeV, $\cancel{E}_T > 80$ GeV) and ($H_T > 225$ GeV, $\cancel{E}_T > 100$ GeV) tight candidate samples.

Background	Loose Sample	Tight Sample
$Z \rightarrow \nu\nu + \text{jets}$	888 ± 54	86 ± 13
$W \rightarrow e\nu + \text{jets}$	669 ± 42	50 ± 8
$W \rightarrow \mu\nu + \text{jets}$	399 ± 25	33 ± 5
$W \rightarrow \tau\nu + \text{jets}$	256 ± 16	14 ± 2
$Z \rightarrow ee + \text{jets}$	0 ± 0	0 ± 0
$Z \rightarrow \mu\mu + \text{jets}$	13 ± 2	1 ± 0
$Z \rightarrow \tau\tau + \text{jets}$	16 ± 2	1 ± 0
Top quark production	74 ± 9	11 ± 2
QCD multi-jet	49 ± 30	9 ± 9
$\gamma + \text{jets}$	75 ± 11	5 ± 1
Non-collision	4 ± 4	1 ± 1
Total expected	2443 ± 145	211 ± 30
Data observed	2506	186

1 5.2. Dijet+ \cancel{E}_T search

As in the case of the monojet analysis, different kinematic regions have been probed in the dijet+ \cancel{E}_T analysis. These regions have been defined in terms of the \cancel{E}_T and the scalar sum of the transverse energy of each of the two jets contained in the event ($H_T = E_T(j_1) + E_T(j_2)$). From the trigger requirement (\cancel{E}_T trigger), the lowest kinematic region is defined as $\cancel{E}_T > 80$ GeV and $H_T > 125$ GeV. We refer to this region as the loose sample. By requiring that there are enough W/Z+jets events to perform a data-driven estimate of the Standard Model contribution to dijet+ \cancel{E}_T events with 2 fb^{-1} of CDF data, a second kinematic region has been defined as $\cancel{E}_T > 100$ GeV and $H_T > 225$ GeV (tight sample). Once again, predictions have been independently obtained for these two regions. Results of the predictions and a comparison with the observed number of dijet+ \cancel{E}_T events are presented in Table 6. The agreement between the observations and the Standard Model predictions are excellent, showing no evidence for new physics. As was done in the monojet analysis, differential distributions were compared to the observed data and the agreement between with Standard Model predictions was again good. Results for the \cancel{E}_T distribution of the loose sample are displayed in Fig. 3.

The results above can be used to constrain any new physics model which predicts a dijet+ \cancel{E}_T signature. A 95% C.L. limit on the number of new physics events in each of the candidate samples is obtained from the number of observed events, the number of predicted Standard Model events and its uncertainty. For the loose region, this upper limit consists of 359 events, while for the tight sample this limit is

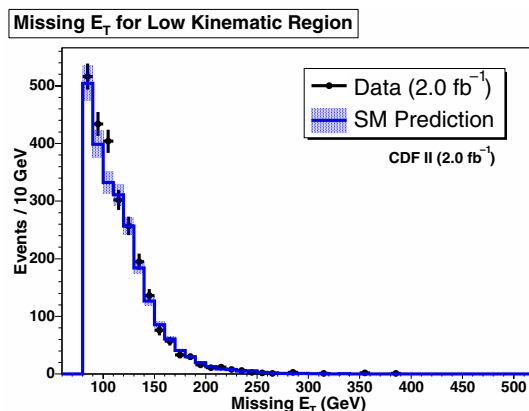


Fig. 3. Comparison of the event \cancel{E}_T for the 2,443 events in the candidate sample used for the loose dijet+ \cancel{E}_T search for new physics with the predicted Standard Model distribution. The prediction does not include a systematic uncertainty on the shape of the Standard Model background distribution which is directly taken from Monte Carlo.

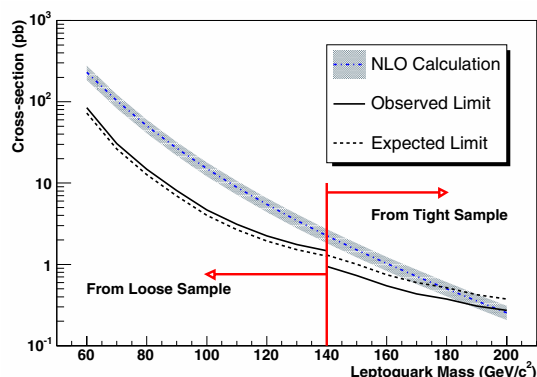


Fig. 4. 95% C.L. cross section limits on first and second generations $q\nu$ scalar leptoquark pair production (q being u , d , s or c) as a function of leptoquark masses M_{LQ} . The lower limit on the leptoquark mass is obtained from the intersection between the observed limit (straight black line) and the NLO calculation (blue dotted line).

1 51 events. After the signal acceptance to dijet+ \cancel{E}_T selection is calculated, the upper
 2 limits on new physics model cross sections can be obtained. Leptoquark models for
 3 which a pair of leptoquarks is produced each decaying to a quark and a neutrino
 4 was chosen for its simplicity: it depends only on two free parameters (the leptoquark
 5 mass and branching ratio), facilitating comparisons with other experimental results.
 6 For each tested leptoquark mass, an *a priori* choice of the kinematic region to be
 7 used for the constraints was made. Up to 140 GeV, constraints have been set from
 8 the loose sample prediction. Results are shown in Fig. 4. As can be seen in the
 9 figure, the mass point for which the 95% C.L. distribution from data crosses the
 leptoquark cross section distribution marks the upper limit set by the dijet+ \cancel{E}_T

1 measurement on the leptoquark mass. This limit of $190 \text{ GeV}/c^2$ corresponds to an
 2 upper limit of 0.31 pb on the leptoquark pair production cross section.

3 **6. Conclusion**

4 Jets-plus- \cancel{E}_T signatures have a lot of potential for discoveries of new physics beyond
 5 the Standard Model. These signatures are predicted in many new physics scenarios
 6 and in some of those models, Dark Matter particles are responsible for the observed
 7 \cancel{E}_T .

8 In order to maximize the sensitivity and robustness of these searches, data-
 9 driven methods were developed and used in measurements performed at the Teva-
 10 tron with the CDF detector. Two examples of such searches were discussed: a
 11 monojet and a dijet+ \cancel{E}_T analysis. The advantage of data-driven background esti-
 12 mates applied in this context in reducing the overall uncertainty and in increasing
 13 the search sensitivity was demonstrated. The CDF searches found no evidence of
 14 physics beyond the Standard Model, and constraints on parameters of new physics
 15 models were obtained. In particular, the monojet analysis set limits on the funda-
 16 mental Planck scale of a large extra dimension model while the dijet+ \cancel{E}_T analysis
 17 was used to set limits on the mass of leptoquarks.

18 The strategies and methods presented in this review and tested at the Tevatron
 19 will hopefully play an important role in future discoveries at the LHC.

Acknowledgments

21 The authors would like to thank Dr. Eric James and Dr. Dan MacQueen for their
 22 help in developing the analyses and techniques described in this review. We also
 23 thank our CDF collaborators, the Fermilab staff and the technical staffs of the
 participating institutions for their vital contributions.

25 References

- 26 1. W.-M. Yao *et al.*, *J. Phys. G* **33**, 1 (2006), also see <http://pdg.lbl.gov>
- 27 2. For example of review, see *TASI Lectures on Precision Electroweak Physics*,
 K. Matchev, UFIFT-HEP-03-11, CLNS-04/1862.
- 28 3. For example of review, see *TASI Lectures on The Strong CP Problem*, M. Dine,
 SCIPP-00/30.
- 29 4. J. L. Feng, *J.Phys. G* **32**, R1 (2006).
- 30 5. CDF Collab. (A. Abulencia *et al.*), *Phys. Rev. Lett.* **97**, 171802 (2006).
- 31 6. CDF Collab. (T. Aaltonen *et al.*), *Phys. Rev. Lett.* **101**, 181602 (2008).
- 32 7. CDF Collab. (T. Aaltonen *et al.*), submitted to *Phys. Rev. Lett.*, arXiv:0912.4691.
- 33 8. G. L. Kane and J. P. Leville, *Phys. Lett. B* **112**, 227 (1982).
- 34 9. P. R. Harrison and C. H. Llewellyn-Smith, *Nucl. Phys. B* **213**, 223 (1983).
- 35 10. I. Antoniadis, N. Arkani-Hamed, S. Dimopoulos and G. Dvali, *Phys. Lett. B* **436**, 257
 (1998).
- 36 11. G. Azuelos, P.-H. Beauchemin and C. P. Burgess, *J. Phys. G: Nucl. Part.* **31**, 1 (2005).
- 37 12. D. Atwood, C. P. Burgess, E. Filotas, F. Leblond, D. London and I. Maksymyk, *Phys.*
 38 *Rev. D* **63**, 025007 (2001).

- 1 13. J. L. Hewett and T. G. Rizzo, *Phys. Rev. D* **56**, 5709 (1997).
14. M. Krämer, T. Plehn, M. Spira and P. M. Zerwas, *Phys. Rev. Lett.* **79**, 341 (1997).
- 3 15. H. Goldberg, *Phys. Rev. Lett.* **50**, 1419 (1983).
16. J. R. Ellis, J. S. Hagelin, D. V. Nanopoulos, K. A. Olive and M. Srednicki, *Nucl. Phys. B* **238**, 453 (1984).
- 5 17. G. Servant and T. M. P. Tait, *Nucl. Phys. B* **650**, 391 (2003).
- 7 18. H. C. Cheng, J. L. Feng and K. T. Matchev, *Phys. Rev. Lett.* **89**, 211301 (2002).
19. H. C. Cheng and I. Low, *JHEP* **0309**, 051 (2003).
- 9 20. CDF Collab. (F. Abe *et al.*), *Phys. Rev. D* **45**, 1448 (1992).
21. A. Bhatti *et al.*, *Nucl. Instrum. Meth. A* **566**, 375 (2006).
- 11 22. J. Campbell and K. Ellis, *Monte carlo for FeMtobarn processes at hadron Colliders*, see <http://mcfm.fnal.gov/>.
- 13 23. G.F. Giudice, R. Rattazzi and J. D. Wells, *Nucl. Phys. B* **544**, 3 (1999).
24. S. Hannestad and G. Raffelt, *Phys. Rev. Lett.* **87**, 051301 (2001).
- 15 25. S. Hannestad and G. Raffelt, *Phys. Rev. Lett.* **88**, 071301 (2002).
26. S. Hannestad and G. Raffelt, *Phys. Rev. D* **67**, 125008 (2003) [Erratum-*ibid.* **69**, 029901 (2004)].
- 17 27. S. Hannestad, *Phys. Rev. D* **64**, 023515 (2001).